ИЗВЕСТИЯ ВЫСШИХ УЧЕБНЫХ ЗАВЕДЕНИЙ.
Т 62 (9) Серия «**ХИМИЯ И ХИМИЧЕСКАЯ ТЕХНОЛОГИЯ**» 2019

IZVESTIYA VYSSHIKH UCHEBNYKH ZAVEDENII
V 62 (9) **KHIMIYA KHIMICHESKAYA TEKHNOLOGIYA** 2019
RUSSIAN JOURNAL OF CHEMISTRY AND CHEMICAL TECHNOLOGY

DOI: 10.6060/ivkkt.20196209.6065

УДК: 544.7:544.478.02:544.478.1

ЭКОЛОГИЧЕСКИ БЕЗОПАСНЫЙ СПОСОБ СИНТЕЗА НИКЕЛЕВЫХ КАТАЛИЗАТОРОВ ГИДРОГЕНИЗАЦИИ

А.Р. Латыпова, Д.В. Филиппов, О.В. Лефедова, А.В. Быков, В.Ю. Долуда

Адель Ришатовна Латыпова *, Дмитрий Вячеславович Филиппов, Ольга Валентиновна Лефедова

Кафедра физической и коллоидной химии, Ивановский государственный химико-технологический университет, просп. Шереметевский, 7, Иваново, Российская Федерация, 153000
E-mail: LatAdel@yandex.ru, Filippov@isuct.ru, physchem.606@yandex.ru

Алексей Владимирович Быков, Валентин Юрьевич Долуда

Кафедра биотехнологии, Тверской государственный технический университет, наб. Афанасия Никитина, 22, Тверь, Российская Федерация, 170026
E-mail: bykovav@yandex.ru, doludav@yandex.ru

Предложены способы получения новых никелевых катализаторов методом поверхностного осаждения многоядерных гидроксокомплексов никеля (II) на порошкообразных носителях с последующим восстановлением до металла. Данная методика является экологически чистой, безопасной и безотходной технологией. Промышленные сточные воды будут содержать только раствор хлорида и карбоната натрия. Катализаторы на различных носителях, таких как SiO_2, γ-Al_2O_3, были получены через осаждение полиядерных гидроксокомплексов (ПГС) никеля (II) на порошкообразные носители, суспендированные в водном растворе Na_2CO_3 с последующим восстановлением соли в токе водорода при 300 °С до металла. Каталитическую активность определяли в условиях реакции гидрирования п-нитроанилина при 240 °С и давлении водорода 40 бар. Катализаторы были охарактеризованы с помощью ТПД аммиака, РФЭС и ИК спектроскопии. Полученные данные свидетельствуют, что при нанесении никеля на носители γ-Al_2O_3 и SiO_2, каталитическая фаза состоит из нескольких оксидов никеля и модификаций его гидроксида. В составе катализатора Ni/γ-Al_2O_3 катализировать процесс могут соединения NiO, NiO, γ-NiOOH и $Ni(OH)_2$, а для Ni/SiO_2 это NiO, NiO, Ni_2O_3, γ-NiOOH и $Ni(OH)_2$. Однако, необходимо проведение предварительной активации катализатора в газовой атмосфере под давлением. Показано, что изменения концентраций в катализаторах до и после использования могут быть связаны с взаимными превращениями модификаций, зависимо или не зависимо от катализа процесса гидрогенизации. Также установлено, что катализатор, нанесенный на гамма оксид алюминия, был в 10 раз активнее, чем катализатор на оксиде кремния.

Ключевые слова: никель, катализатор, экология, гидргенизация, анилин, нитробензол, спилловер водорода

Для цитирования:
Латыпова А.Р., Филиппов Д.В., Лефедова О.В., Быков А.В., Долуда В.Ю. Экологически безопасный способ синтеза никелевых катализаторов гидрогенизации. *Изв. вузов. Химия и хим. технология*. 2019. Т. 62. Вып. 9. С. 46–52

For citation:
Latypova A.R., Filippov D.V., Lefedova O.V., Bykov A.V., Doluda V.Yu. Environmentally safe synthesis of hydrogenation nickel catalysts. *Izv. Vyssh. Uchebn. Zaved. Khim. Khim. Tekhnol*. 2019. V. 62. N 9. P. 46–52

ENVIRONMENTALLY SAFE SYNTHESIS OF HYDROGENATION NICKEL CATALYSTS

A.R. Latypova, D.V. Filippov, O.V. Lefedova, A.V. Bykov, V.Yu. Doluda

Adele R. Latypova*, Dmitry V. Filippov, Olga V. Lefedova

Department of Physical and Colloidal chemistry, Ivanovo State University of Chemistry and Technology, Sheremetievskiy ave., 7, Ivanovo, 153000, Russia
E-mail: LatAdel@yandex.ru*, Filippov@isuct.ru, physchem.606@yandex.ru

Alexey V. Bykov, Valentin Yu. Doluda

Department of Biotechnology, Tver State Technical University, Afanasy Nikitin Embankment, 22, Tver, 170026, Russia
E-mail: bykovav@yandex.ru, doludav@yandex.ru

New types of nickel catalysts are proposed. They are formed during the surface deposition of nickel polynuclear hydroxo complexes on powdered carriers with subsequent reduction to the metal. This method of synthesis is environmentally friendly, safe and waste-free technology. Industrial wastewater will contain only an aqueous solution of sodium chloride and sodium carbonate. The catalytic activity was determined by the p-nitroaniline hydrogenation at 240 °C and 40 bar of hydrogen pressure. The properties and characteristics of the catalysts were studied using thermo-programmable desorption of ammonia, Fourier-transform infrared spectroscopy and X-ray photoelectron spectroscopy. It was found that Ni/γ-Al_2O_3 catalyst may accelerate the process with NiO, NiO, γ-NiOOH and $Ni(OH)_2$ compounds, while for Ni/SiO_2 these are NiO, NiO, Ni_2O_3, γ-NiOOH and $Ni(OH)_2$. However, pre-activation of the sample is necessary. The solution of this problem can be the catalyst activation in a gas atmosphere under hydrogen pressure, but at a lower temperature of about 250 °C. Changes in the metal content in the catalysts before and after use may be associated with the mutual transformations of modifications, which may or may not depend on the catalysis of the hydrogenation process. We established that the catalyst supported on gamma alumina was 10 times more active than the catalyst on silicon oxide. The discovery of the mechanism of transformations between modifications of oxides and metal hydroxides is of considerable interest in the development of new selective and environmentally friendly catalysts.

Key words: nickel, catalyst, ecology, industry, hydrogenation, aniline, nitrobenzene, hydrogen spillover

INTRODUCTION

When developing modern producing catalysts methods, it is necessary to invest heavily in solving such problems as reliable waste disposal [1-3]. In addition, to obtain new catalytic materials are increasingly used organic solvents, causing significant damage to the environment [4, 5]. Therefore, the development of simple, environmentally friendly and non-waste technologies seems to be a very urgent task [6-8]. In this regard, the cost of the resulting industrial catalysts is also an important factor. The high cost of platinum group metals causes a growing interest in more affordable nickel, iron or manganese. Recently, in scientific periodicals, there has been a noticeable tendency to search for new efficient heterogeneous and homogeneous catalysts based on nickel and manganese [9-12]. The aim of the work is to acquaint the authors with the results of obtaining and screening new types of catalysts.

EXPERIMENTAL PART

2.1. Chemicals and materials

Silica was synthesized by the sol-gel method. We used chemically pure tetraethoxysilane (99.9% Vekton, Russia), 2-propanol (99% Vekton, Russia), sodium carbonate (Vekton, Russia), nickel chloride (Vekton, Russia). Other reagents were analytically pure and were used without further purification. High purity gases (N_2 99.99%; H_2 99.99%) were applied to prepare the catalyst.

2.2. Silica sol-gel synthesis

To prepare spherical silica nanoparticles, 700 ml of distilled water was added to 500 ml of 2-propanol. Then 200 ml of tetraethoxysilane solution was poured. Thereafter, 50 ml of ammonia solution was added dropwise to the reaction mixture over 30 min. The resulting solution was kept for 120 min with stirring at a speed of 1000 rpm. Then, the resulting sol was filtered, washed with distilled water and dried at 200 °C for 3 h in air.

2.3. Catalyst preparation

The nickel catalyst was prepared by adding dropwise a hydrochloric acid solution of $NiCl_2$ to the carrier powder suspended in an aqueous solution of Na_2CO_3. The mixture was stirred for 3 h at 35 °C. The catalyst was filtered, thoroughly washed with distilled water and dried at 65 °C in air. The resulting sample was activated in a tubular flow reactor in a stream of hydrogen at 300 °C for 60 min. After that, the catalyst was cooled in an atmosphere of hydrogen to room temperature. Hydrogen adsorbed on the catalyst surface was removed by flushing the reactor with nitrogen for 30 min.

2.4. Catalyst characterization

2.4.1. NH_3 TPD

Ammonia temperature-programmed desorption was used to determine the number of acid sites of carriers and catalysts, in particular, γ-alumina. The study was performed using an AutoChem HP 2950 Micromeritics automated chemisorption analyzer. The samples were placed in a U-shaped tube in a muffle furnace, degassed in a helium stream at 900 °C, the sample was cooled to room temperature and then treated with a steady stream of gas mixture 3 volume % NH_3/He. The ammonia excess was removed by a helium stream at 25 °C. The analysis was performed with linear heating of samples in a helium flow at a rate of 10 °C per minute from ambient temperature to 900 °C.

2.4.2 FTIR-spectroscopy

IR spectra were used to analyze the surface functional groups of carriers and catalysts. They were obtained using a Shimadzu IRPrestige-21 IR Fourier spectrometer with an infrared Fourier transform and a resolution of 0.5 cm^{-1}.

2.4.3 XPS

The XPS spectra of the catalysts were obtained using an ES-2403 spectrometer (manufacturer: Institute for Analytical Instrumentation, RAS, St. Petersburg, Russia), Mg Kα radiation (hν=1253.6 eV). The device is equipped with a PHOIBOS 100-MCD5 energy analyzer (SPECS GmbH, Germany) and an XR-50 X-ray source (SPECS, Germany). All studies were performed at an X-ray power of 250 watts. The survey spectra were performed with an energy step of 0.5 eV, and high-resolution spectra were recorded with an energy step of 0.05 eV.

2.4.4. Catalytic tests

The nitrobenzene hydrogenation reaction was carried out in an autoclave (volume 100 ml) of a Multiple Reactor System 5000. The catalyst known amount was dispersed in 10 ml of 2-propanol or hexane, and then 2 ml of nitrobenzene was added. Hexane was used in the case of studying the effect of solvent on the catalyst activity and selectivity. The autoclave was sealed, purged with nitrogen, heated to the required temperature with magnetic stirring at a speed of 1000 rpm. The system was purged three times with hydrogen at a pressure of 15 bar and, before the start of the experiment the pressure of hydrogen was raised to 40 bar. Throughout all the studies, probes were taken from the reaction mixture at regular intervals. Qualitative and quantitative analysis was performed using a gas chromatograph (Crystal Lux 4000M, manufacturer Meta-Chrom). The reaction rate was controlled through the nitrobenzene conversion. After the process completion the reactor was cooled to room temperature, the pressure was vented through a special valve. The catalyst was separated from the reaction mixture by centrifugation.

RESULT AND DISCUSSION

3.1. IR spectra of carriers and catalysts

Analysis of the both oxides FTIR spectra showed that wide bands with a center of about 3420-3468 cm^{-1} correspond to vibrations of water molecules linked by a hydrogen bond (O–H). On the other hand, the stretching vibrations of hydrogen-bonded surface silanols (SiO-H) appear at 3451-3471 cm^{-1} [13].

The use of tetraethyl orthosilane as a precursor of silica led to the surface methyl functionalized silicon dioxide formation. The corresponding infrared spectra show several peaks in the range of 1338, 1431 cm^{-1}, corresponding to the $-CH_3$ and $>CH_2$ groups deformation vibrations [13, 14]. Intense bands that appear at 1059-1176 cm^{-1} are related to Si-O-Si asymmetric stretching vibrations. Symmetric stretching vibrations of Si-O-Si, O-Si-O deformational vibrations, Si-O flat stretching vibrations can overlap in the range of 430-953 cm^{-1}. Usually, Si-O stretching vibration bands indicate defects in the atomic oxide lattice [13, 14]. In the SiO_2 FTIR spectra the absorption bands of the adsorbed water molecules deformation vibrations appear at 1338, 1431, 1632 cm^{-1} [13, 14].

In the γ-Al_2O_3 IR spectra the absorption bands of the adsorbed water molecules deformation vibrations appear at 1533, 1641 cm^{-1}. The signal is observed at 2114 cm^{-1}, it refers to the deformation vibrations of carboxyl groups.

Thus, the aluminum oxide surface can be coated with covalently bound carboxyl groups (absorption bands at 785 cm^{-1}) [15, 16]. The antisymmetric stretching vibration of Al-O-Al and the stretching vibration of Al-OH can be observed at 785 cm^{-1} and 1022 cm^{-1}. The absorption band at 3470 cm^{-1} refers to the stretching vibrations of the carrier OH groups and the partially adsorbed alcohol. The latter assumption is confirmed by the presence of deformation vibrations at 1387 cm^{-1}, corresponding to the $–CH_3$ and $>CH_2$ groups [16].

The spent catalysts IR spectra showed the presence on the surface of materials both the starting compound – nitrobenzene and its hydrogenation product – aniline. The NH_2 group valence vibrations appeared at 3371 and 3218 cm^{-1}. The bands at 1603 cm^{-1} were observed, which indicates the presence of vibrations of the N–H bond [17]. The band at 1381 cm^{-1} was attributed to the deformation vibrations of the CH, CH_2, and CH_3 groups. The valent C–H vibrations of the benzene ring correspond to bands at 3070 and 3024 cm^{-1} [16, 17]. And the absorption bands at 1342 cm^{-1} and 1515 cm^{-1} were attributed to the symmetric and antisymmetric stretching NO_2 group vibrations [17].

3.2. XPS study of fresh and spent catalysts

The spectra of the catalyst on aluminum oxide showed the presence of the following elements on the surface: Al (31%), O (45%), Ni (13%), C (11%), Cl (0.2%) and F (0.3%). The catalyst surface on silica contains elements with atomic concentration: Si (29%), O (53%), C (12%), Ni (1.5%), Na (4.5%), Cl (0.2%) and F (0.2%). According to the spectra of the used catalysts, the nickel content in the sample 5% $Ni/\gamma\text{-}Al_2O_3$ decreased to 6.4% and in the sample 5% Ni/SiO_2 to 0.5%. The metal significantly lower amount on the surface indicates that in the case of porous silica a large part of the catalytic phase formed in the volume of the porous space. The high resolution spectra of the catalysts on both carriers showed that the catalytic phase consists of the same components: Ni^o, NiO, Ni_2O_3, $Ni(OH)_2$ (consists of $\alpha\text{-}Ni(OH)_2$ и $\beta\text{-}Ni(OH)_2$) and γ-NiOOH, β-NiOOH [18-20] – Table 1,2. The separation in the $Ni(OH)_2$ spectrum into the components $\alpha\text{-}Ni(OH)_2$ and $\beta\text{-}Ni(OH)_2$ is difficult due to the lack of reference information of the X-ray photoelectron spectra of these compounds. It is difficult to isolate these individual components in pure form. It is known that nickel is easily oxidized even by atmospheric oxygen with the formation of various oxides and hydroxides, which can exhibit catalytic activity under conditions of high temperature and pressure [21].

Table 1

$Ni/\gamma\text{-}Al_2O_3$ XPS study results

***Таблица 1.* Данные РФЭС для катализатора $Ni/\gamma\text{-}Al_2O_3$**

Component	Nickel atomic fraction on the surface, %		
	before activation	after activation	spent catalyst
Ni^0	2.90	2.90	2.10
NiO	13.5	25.2	7.80
Ni_2O_3	35.4	9.10	69.3
γ-NiOOH	25.8	21.3	6.50
β-NiOOH	18.7	0	3.50
$Ni(OH)_2$	3.80	41.5	10.8

Table 2

Ni/SiO_2 XPS study results

***Таблица 2.* Данные РФЭС для катализатора Ni/SiO_2**

Component	Nickel atomic fraction on the surface, %		
	before activation	after activation	spent catalyst
Ni^o	2.80	2.20	0.50
NiO	16.1	15.7	2.20
Ni_2O_3	39.1	10.6	5.70
γ-NiOOH	17.1	46.5	81.9
β-NiOOH	6.00	5.40	0
$Ni(OH)_2$	18.9	19.6	9.70

According to the literature, mutual transformations are possible between these forms [22, 23]:

- $\alpha\text{-}Ni(OH)_2$ is converted to $\beta\text{-}Ni(OH)_2$ by dehydrogenation;
- β-NiOOH, being oxidized, can also turn reversibly into γ-NiOOH;
- $\alpha\text{-}Ni(OH)_2$ is reversibly oxidized to γ-NiOOH, and $\beta\text{-}Ni(OH)_2$ to β-NiOOH, respectively.

Thus, from the data in Tables 1 and 2, it can be assumed that on the $Ni/\gamma\text{-}Al_2O_3$ catalyst Ni_2O_3 oxide is formed by the sequential oxidation of $\alpha\text{-}Ni(OH)_2$ to γ-NiOOH and γ-NiOOH to Ni_2O_3. Ni^o and NiO also contributed to the formation of trivalent nickel oxide. The presence of $\beta\text{-}Ni(OH)_2$ can be confirmed by the fact that after catalysis a small amount of its oxidation product β-NiOOH has formed on the surface. The 5% Pd/SiO_2 catalyst differs from the $Ni/\gamma\text{-}Al_2O_3$ catalyst in that in the activated and treated catalyst the greatest concentration of the γ-NiOOH component was observed, which probably was formed from β-NiOOH and $\alpha\text{-}Ni(OH)_2$ immediately after activation due to oxidation by air oxygen. In the process of catalysis, β-NiOOH and $\alpha\text{-}Ni(OH)_2$ continue to oxidize completely or partially to γ-NiOOH and, apparently, the components Ni^0, NiO, Ni_2O_3 are also capable of forming γ-nickel-oxyhydroxide under conditions of pressure hydrogenation at high temperatures. Although predicting the mechanism of these transformations is still very difficult.

A comparative analysis of the high-resolution spectra of the catalysts $Ni/\gamma\text{-}Al_2O_3$ and Ni/SiO_2 before and after use showed that in the case of the catalyst on alumina there was a slight decrease in the total metal content, whereas in the case of the catalyst on silica, the decrease in the metal phase on the material surface was significant.

This may be due to the strong carburization of the surface, because carbon content on the catalyst surface increased from 12 to 47 atomic fractions.

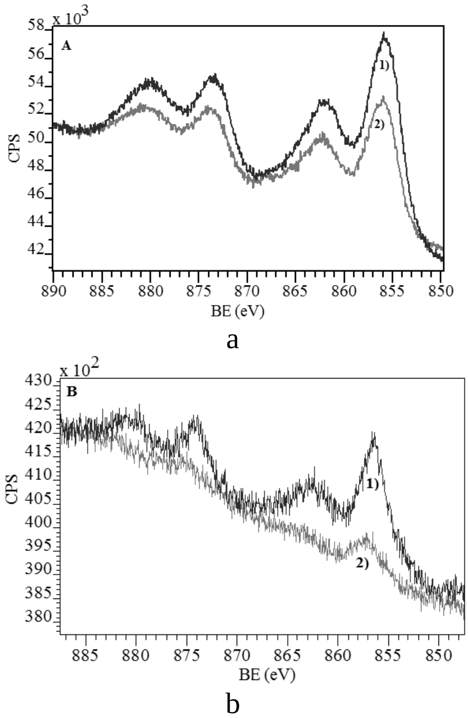

a

b

Fig. 1. High-resolution spectra for fresh (1) and spent (2) catalysts: a) Ni/γ-Al_2O_3 b) Ni/SiO_2

Рис. 1. Спектры высокого разрешения Ni 2p для (1) исходного и (2) отработанного: a) Ni/γ-Al_2O_3 b) Ni/SiO_2

3.3. Nitrobenzene hydrogenation kinetics

The investigation of nitrobenzene hydrogenation kinetics on a 5% Ni/γ-Al_2O_3 catalyst at a temperature of 513 K and a hydrogen pressure of 40 atm was carried out. The results showed that the catalyst is additionally activated under hydrogen pressure for half an hour and fully converts nitrobenzene to aniline over the next 1.5 hours (Fig. 2). This is faster than hydrogenation on the same catalyst at a temperature of 493 K and a pressure of 40 atm. However, in the latter case, the reaction is catalyzed from the first minutes of the experiment (Fig. 3).

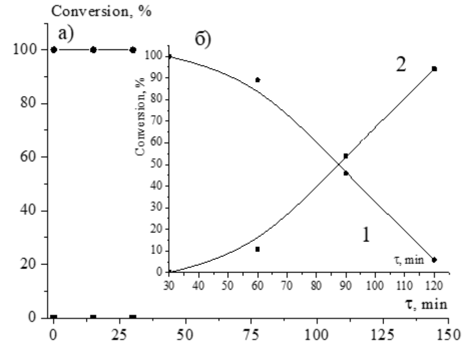

Fig. 2. Nitrobenzene hydrogenation kinetic curves on 5% Ni/γ-Al_2O_3 catalyst in 2-propanol at 40 bar and 513 K. 1 – nitrobenzene; 2 – aniline. a) additional activation stage, b) the kinetic curves

Рис. 2. Кинетические кривые гидрогенизации нитробензола на 5% Ni/γ-Al_2O_3 в 2-пропаноле при 40 атм. и 513 K. 1 – нитробензол; 2 – анилин. a) дополнительная стадия активации b) кинетические кривые

Perhaps in the course of the experiment, the nitrobenzene content in the vapor phase increases with increasing temperature. Then, the free surface fraction and hydrogen adsorption increase. The metal is activated easily interacting with hydrogen at high temperatures and gas pressure. This assumption may explain the observed phenomenon.

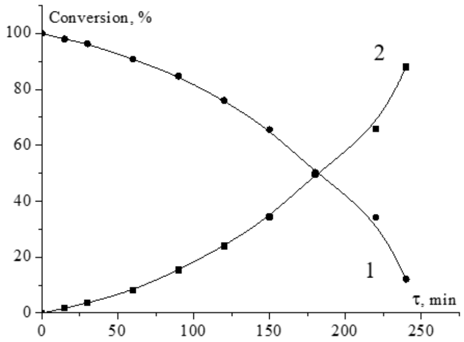

Fig. 3. Nitrobenzene hydrogenation kinetic curves on 5% Ni/γ-Al_2O_3 catalyst in 2-propanol at 40 bar and 493 K. 1 – nitrobenzene; 2 – aniline

Рис. 3. Кинетические кривые гидрогенизации нитробензола на 5% Ni/γ-Al_2O_3 в 2-пропаноле при 40 атм. и 493 K. 1 – нитробензол; 2 – анилин

Comparison of catalysts on aluminum oxide and silica showed that the first carrier is better. The catalyst activity on silica is ten times lower (Table 3).

Table 3

Kinetics of nitrobenzene hydrogenation with various catalysts at different temperatures and solvents

***Таблица 3.* Кинетика гидрирования нитробензола на различных катализаторах при разных температурах и растворителях**

Catalyst	T, K	Solvent	rate, $sec^{-1}\cdot g^{-1}$
5% Ni/γ-Al_2O_3	423	2-propanol	0.78
5% Ni/γ-Al_2O_3	473	2-propanol	2.33
5% Ni/γ-Al_2O_3	493	2-propanol	2.09
5% Ni/γ-Al_2O_3	513	2-propanol	6.93
5% Ni/γ-Al_2O_3	513	hexane	1.43
5% Ni/SiO_2	240	2-propanol	0.69

It is interesting to note that under the same conditions (513 K and 40 atm. of hydrogen), nitrobenzene hydrogenation on a 5% Ni/SiO_2 catalyst was also observed before the catalyst was activated (Fig. 4).

Moreover, the 5% Ni/SiO_2 is activated under hydrogen pressure on average, an hour more than Ni/γ-Al_2O_3. This is explained by the difference in the morphology of the materials surface. There is an opinion according to which a two-center model of adsorption is observed on metal centers fixed on the amorphous surface of the carrier, whereas when used as a carrier of materials with crystal architecture, there is a one-center model. Due to this, the catalysts on such carriers have a higher degree of surface utilization efficiency and higher activity. Thus, γ-Al_2O_3 has a crystalline surface structure and very well adsorbs hydrogen, which as a result of spillover can flow into the metal phase and participate in the hydrogenation process. While SiO_2 has an amorphous and porous structure, for which the flow of spillover is unlikely. Therefore, the activity of the catalyst on it below. In addition, during the formation of the catalytic phase of nickel in the porous structure of the carrier, the hydrogen diffusion process negatively affects the reaction kinetics.

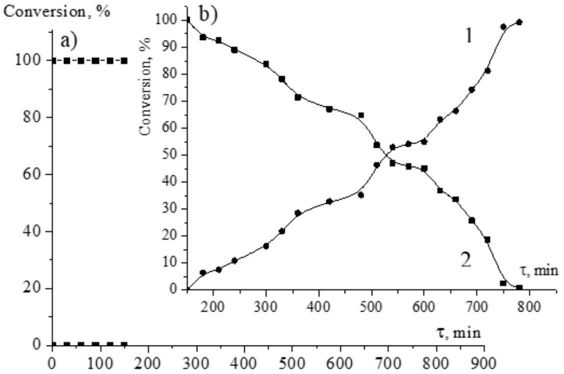

Fig. 4. Nitrobenzene hydrogenation kinetic curves on 5% Ni/SiO_2 in 2-propanol at 40 bar and 513 K. 1 – nitrobenzene; 2 – aniline
Рис. 4. Кинетические кривые гидрогенизации нитробензола на 5% Ni/SiO_2 в 2-пропаноле при 40 атм. и 513 K. 1 – нитробензол; 2 – анилин

Table 4

Selectivity of various catalysts in hydrogenation of nitrobenzene to aniline at different temperatures and solvents
Таблица 4. Селективность различных катализаторов гидрогенизации нитробензола до анилина при различных температурах и растворителях

Catalyst	T, K	Nitrobenzene	Aniline	Other Products
5% Ni/γ-Al_2O_3	423	70.5	~ 29	~ 0.5
5% Ni/γ-Al_2O_3	473	11.2	~ 88.4	~ 0.4
5% Ni/γ-Al_2O_3	493	12.1	87.3	~ 0.6
5% Ni/γ-Al_2O_3	513	5.9	~ 93.3	~ 0.8
5% Ni/γ-Al_2O_3	513*	7	93	0
5% Ni/SiO_2	240	0.8	99.2	0

Note: * Nitrobenzene hydrogenation in hexane at 40 bar and 513 K

Примечание: * Гидрирование нитробензола в гексане при 40 атм. и 513 K

The results of the study of the solvent influence confirmed the hypothesis that an aprotic solvent increases the selectivity of hydrogenation under pressure. This is consistent with the fact that the activity of the catalysts is lower in an aprotic solvent. It is obvious that the proton solvent can be a source of hydrogen. This has a positive effect on activity and negatively on the selectivity of the catalyst with respect to aniline (Tables 3, 4).

CONCLUSION

Various modifications and varieties of aluminum oxide are widely used for the preparation of catalysts, whereas similar modifications of nickel oxides and hydroxides have not yet found their use in catalysis. According to the data obtained, when nickel is deposited on γ-Al_2O_3 and SiO_2 carriers, the catalytic phase consists of several nickel oxides and its hydroxide modifications. From the information on changes in the various components content, we can assume which of them are involved in catalysis, and which are not. It is likely that Ni/γ-Al_2O_3 catalyst may accelerate the process with Ni^{O}, NiO, γ-NiOOH and $Ni(OH)_2$ compounds, while for Ni/SiO_2 these are Ni^{O}, NiO, Ni_2O_3, γ-NiOOH and $Ni(OH)_2$. However, the need to pre-treat catalysts with hydrogen under pressure should be taken into account. The solution of this problem can be the catalyst activation in a gas atmosphere under hydrogen pressure, but at a lower temperature of about 250 °C.

Changes in the metal content in the catalysts before and after use may be associated with the mutual transformations of modifications, which may or may not depend on the catalysis of the hydrogenation process. The last question should be studied in more detail. The discovery of the transformations mechanism between modifications of oxides and metal hydroxides is of considerable interest in the development of new selective and environmentally friendly catalysts. Regarding the choice of carrier, it should be said that the catalyst deposited on gamma alumina is 10 times more active than the catalyst on silica.

This work is supported by the Russian Science Foundation under grant №18-79-10157.

REFERENCES
ЛИТЕРАТУРА

1. **Zhang L., Wu W., Zhang Y., Zhou X.** Clean synthesis gas production from municipal solid waste via catalytic gasification and reforming technology. *Catal. Today.* 2018. V. 318. P. 39–45. DOI: 10.1016/j.cattod.2018.02.050.
2. **Ghayur A., Verheyen T.V., Meuleman E.** Biological and chemical treatment technologies for waste amines from CO_2 capture plants. *J. Environ. Manage.* 2019. V. 241. N 1. P. 514–524. DOI: 10.1016/j.jenvman.2018.07.033.
3. **Cheng J., Zhou F., Xuan X., Liu J., Zhou J., Cen K.** Cascade chain catalysis of coal combustion by Na-Fe-Ca composite promoters from industrial wastes. *Fuel.* 2016. V. 181. P. 820–826. DOI: 10.1016/j.fuel.2016.05.064.
4. **Wang J., Yuan Z., Nie R., Hou Z., Zheng X.** Hydrogenation of nitrobenzene to aniline over silica gel supported nickel catalysts. *Ind. Eng. Chem. Res.* 2010. N 49. P. 4664–4669. DOI: 10.1021/ie1002069.

5. **Tsvetkova I.B., Matveeva V.G., Doluda V.Y., Bykov A.V., Sidorov A.I.** Pd(II) nanoparticles in porous polystyrene: Factors influencing the nanoparticle size and catalytic properties. *J. Mater. Chem.* 2012. V. 22. N 13. P. 6441–6448. DOI: 10.1039/c2jm30634d.
6. **Huo X., Van Hoomissen D.J., Liu J., Vyas S., Strathmann T.J.** Hydrogenation of aqueous nitrate and nitrite with ruthenium catalysts. *Appl. Catal. B Environ.* 2017. V. 211. P. 188–198. DOI: 10.1016/j.apcatb.2017.04.045.
7. **Dyson P.J., Kiwi-Minsker L., Beswick O., Oberson L., Muriset F., Sulman E., LaGrange T., Lamey D., Yoon S.** Ni-based structured catalyst for selective 3-phase hydrogenation of nitroaromatics. *Catal. Today.* 2016. V. 273. P. 244–251. DOI: 10.1016/j.cattod.2016.04.020.
8. **He L., Niu Z., Miao R., Chen Q., Guan Q., Ning P.** Selective hydrogenation of phenol by the porous Carbon/ZrO_2 supported Ni–Co nanoparticles in subcritical water medium. *J. Clean. Prod.* 2019. V. 215. P.375–381. DOI: 10.1016/j.jclepro.2019.01.077.
9. **Hutchings G.J., Van Der Riet M., Hunter R.** CO Hydrogenation using Cobalt / Manganese Oxide Catalysts. *J. Chem. Soc. Faraday Trans.* 1989. V. 85. P. 19892875–2890. DOI: 10.1039/F19898502875.
10. **Battilocchio C., Hawkins J.M., Ley S.V.** Mild and selective heterogeneous catalytic hydration of nitriles to amides by flowing through manganese dioxide. *Org. Lett.* 2014. V. 16. P. 1060–1063. DOI: 10.1021/ol403591c.
11. **Adkins H., Cramer H.I.** The use of nickel as a catalyst for hydrogeneration. *J. Am. Chem. Soc.* 1930. V. 52. P. 4349–4358. DOI: 10.1021/ja01374a023.
12. **Qi S.C., Zhang L., Einaga H., Kudo S., Norinaga K., Ichiro Hayashi J.** Nano-sized nickel catalyst for deep hydrogenation of lignin monomers and first-principles insight into the catalyst preparation. *J. Mater. Chem. A.* 2017. V. 5. P. 3948–3965. DOI: 10.1039/c6ta08538e.
13. **Al-Oweini R., El-Rassy H.** Synthesis and characterization by FTIR spectroscopy of silica aerogels prepared using several $Si(OR)_4$ and $R''Si(OR')_3$ precursors. *J. Mol. Struct.* 2009. V. 919. P. 140–145. DOI: 10.1016/j.molstruc.2008.08.025.
14. **Beganskienė A., Sirutkaitis V., Marytė kurtinaitienė R.J., Kareiva A.** FTIR. TEM and NMR Iinvestigations of Stöber Silica Nanoparticles. *Mater. Sci.* 2003. V. 10. P. 1392–1320. DOI: 10.1.1.451.9388.
15. **Jafar Tafreshi M., Masoomi Khanghah Z.** Infrared spectroscopy studies on sol-gel prepared alumina powders. *Medziagotyra*. 2015. V. 21. P. 28–31. DOI: 10.5755/j01.ms.21.1.4872.
16. **Saikia B.J., Parthasarathy G.** Fourier transform infrared spectroscopic characterization of kaolinite from Assam and Meghalaya. *Northeast. India. J. Mod. Phys.* 2010. V. 01. P. 206–210. DOI: 10.4236/jmp.2010.14031.
17. **El Khadem H.S.** Spectrometric identification of organic compounds. *J. Chem. Educ.* 1975. V. 52. P. 334. DOI: 10.1021/ed052pA334.2.
18. **Lu X., He J., Jing R., Tao P., Nie R., Zhou D., Xia Q.** Microwave-activated Ni/carbon catalysts for highly selective hydrogenation of nitrobenzene to cyclohexylamine. *Sci. Rep.* 2017. V. 7. P. 1–11. DOI: 10.1038/s41598-017-02519-0.
19. **Grosvenor A.P., Biesinger M.C., Smart R.S.C., McIntyre N.S.** New interpretations of XPS spectra of nickel metal and oxides. *Surf. Sci.* 2006. V. 600. P. 1771–1779. DOI: 10.1016/j.susc.2006.01.041.
20. **Gerson A., Biesinger M.C., Smart R.S.C., Payne B.P., Lau L.W.M.** X-ray photoelectron spectroscopic chemical state quantification of mixed nickel metal. oxide and hydroxide systems. *Surf. Interface Anal.* 2009. V. 41. P. 324–332. DOI: 10.1002/sia.3026.
21. **Pinnel M.R.** Oxidation of nickel and nickel-gold alloys in air at 50°–150°C. *J. Electrochem. Soc.* 2006. V. 126. P. 1274. DOI: 10.1149/1.2129256.
22. **Miao C., Zhu Y., Huang L., Zhao T.** The relationship between structural stability and electrochemical performance of multi-element doped alpha nickel hydroxide. *J. Power Sources*. 2015. V. 274. P. 186–193. DOI: 10.1016/j.jpowsour.2014.10.058.
23. **Huang J.-J., Hwang W.-S., Weng Y.-C., Chou T.-C.** Transformation characterization of $Ni(OH)_2$/NiOOH in Ni-Pt films using an electrochemical quartz crystal microbalance for ethanol sensors. *Mater. Trans.* 2010. V. 51. P. 2294–2303. DOI: 10.2320/matertrans.m2010079.

Поступила в редакцию 20.05.2019
Принята к опубликованию 16.07.2019

Received 20.05.2019
Accepted 16.07.2019